`Sign convention for the Dzyaloshinskii-Moriya Interaction

The chirality of the magnetization texture is determined by the sign of DMI. We are using the convention that positive DMI gives rise to clockwise rotation of the spins corresponding to a right-handed chirality, Fig. S1. With this convention, two interfaces, which induce the same chirality (same DMI sign), increase the total DMI value of the multilayer stack, whereas two interfaces, that induce the opposite chirality (opposite DMI signs), reduce the total DMI value.

Clockwise rotation, D>0, right-handed chirality:

Counterclockwise rotation, D<0, left-handed chirality:

Figure S1: Illustration of the convention used in this paper between the sign of DMI, the rotation of the spins and the chirality.

X-ray analysis of the crystal structure:

We used x-ray diffraction to determine the change of the in-plane lattice constant during the oxidation process. The results are shown in Fig. S2. The oxidation continuously strains the lattice, which is more pronounced for the Pt/$Co_{90}Fe_{10}$ series than for the control series. After oxidation for 1000 s the in-plane lattice constant for both sample series are equal within error bars.

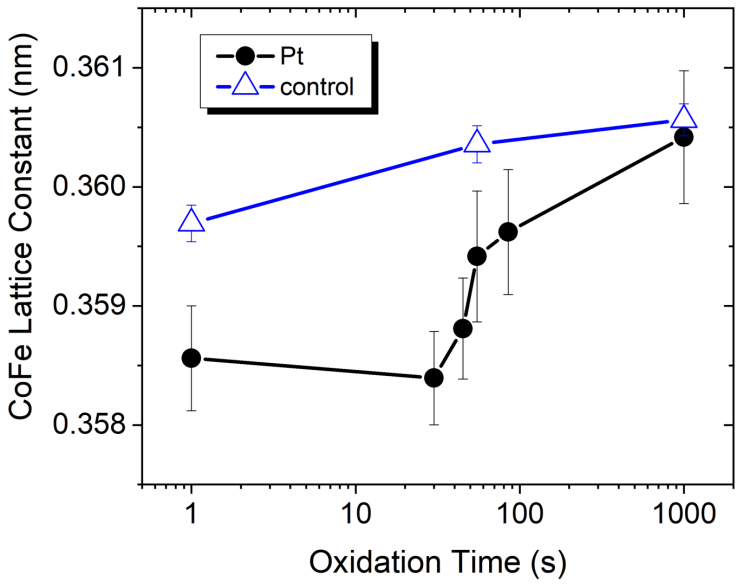

Figure S2: In-plane lattice constant determined by x-ray diffraction for both sample series.

Determination of the difference of the interface anisotropy ΔK between the top and the bottom interfaces

The calculation of the non-reciprocal frequency-shift f_{NR} due to the non-uniform amplitude of the Damon-Eshbach spinwaves through the thickness of the ferromagnet requires the difference of the interface anisotropy between the top and bottom interface ΔK, see eq. 4 in the main part. In the following, we will assume for simplicity that all anisotropy originates from the interface, implying that the volume anisotropy of the $Co_{90}Fe_{10}$ layer is zero. The unoxidized sample of the Cu/$Co_{90}Fe_{10}$ series has Cu on both interfaces of the ferromagnet. Under the assumption that both interfaces are identical, we can obtain the interfacial anisotropy K_{Cu} for the Cu interface from M_{eff} and M_s measured by FMR and SQUID, respectively. During the oxidation the interfacial anisotropy of the top interface changes, see Fig. 3 in the manuscript. Moreover, the knowledge of K_{Cu} allows us to determine the interface anisotropy for the Pt interface K_{Pt} and the change of the anisotropy of the respective oxide interfaces with oxidation time. We are using these interface anisotropy values to calculate the anisotropy induced frequency shift with Eq. 4.

Dependence of the thickness *t* of the ferromagnet on the oxidation

We determined the thickness of the ferromagnet by measuring the magnetic moment with SQUID magnetometry. The unoxidized samples are chosen as a reference to determine the saturation magnetization M_s based on the nominal thickness of 2 nm of the $Co_{90}Fe_{10}$ layer. Any changes of the measured magnetic moment with oxidation time is attributed to a change in thickness, while M_s remains constant. The results are shown in Fig. S3.

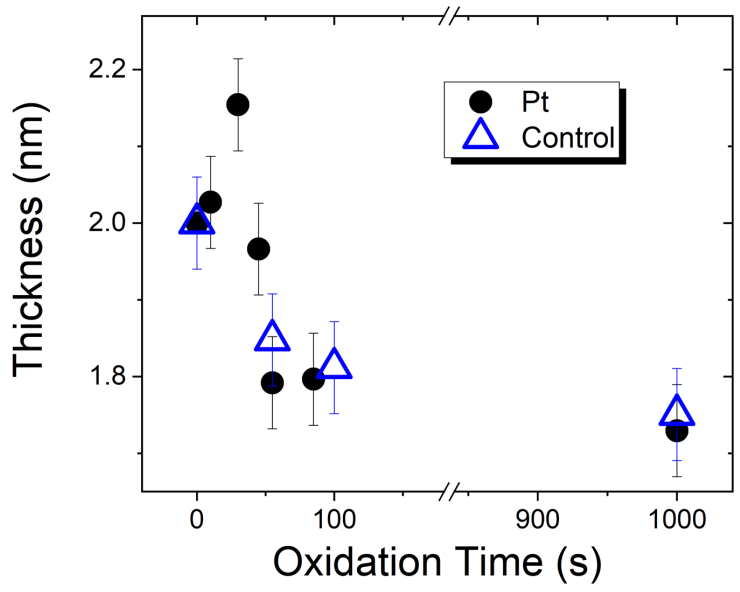

Figure S3: Reduction of the thickness of the ferromagnet with increasing oxidation time.

Not normalized DMI

The DMI is an interface effect and as such the volume averaged value depends on the thickness for the ferromagnet. We show in the manuscript the DMI D^{norm}, which is normalized to a thickness of 1 nm. Here, we provide for comparison the not normalized DMI values D_{DMI}, see Fig. S4 a) and b). It can be seen, that the correlation between the DMI and $g^{\perp}$ does not depend on the normalization. The Pearson correlation coefficient for the not normalized DMI values are $r_s^{Pt} = -0.88$ and r_s^{Cu} =-0.98.

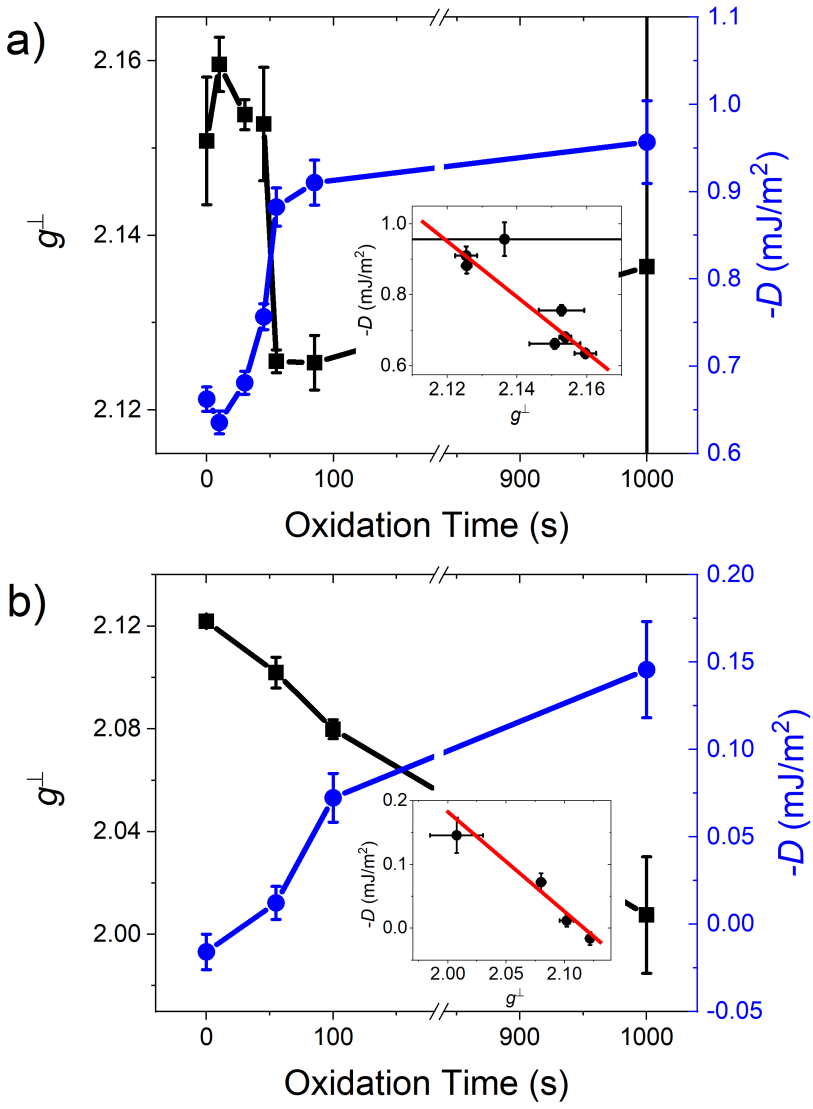

Figure S4: $g^{\perp}$ and D for *a) the Pt/$Co_{90}Fe_{10}$ and b) for the Cu/$Co_{90}Fe_{10}$ sample.*

Ferromagnetic Resonance measurements

The FMR spectra were measured with a Vector-Network-Analyzer (VNA) at fixed frequency while sweeping the magnetic field. In Fig. S5 a) the frequency dependence of the resonance field for the $Cu/Co_{90}Fe_{10}$ control sample without any oxidation is shown together with a fit to the Kittel equation, see eq. 2 in the manuscript. The inset shows the measured real part of the S21 transmission for 16.5 GHz and a fit to the real part of complex susceptibility. Details of the measurement and data analysis procedure can be found in Ref. [24]. The spectroscopic g-factor was determined using an asymptotic analysis outlined in Ref. [23], see Fig. S5 b), where the analysis is shown for the $Pt/Co_{90}Fe_{10}$ sample, which was oxidized for 55s. In short, the resonance field is fitted over many frequency ranges with a lower bound f_{low} and an upper bound f_{up}. The obtained g-factor is then plotted vs.$1/f_{up}^2$ for multiple values of f_{low}. The reported g-factor is the average value of the y-intercepts and the error is determined by the standard deviation of the y-intercepts.

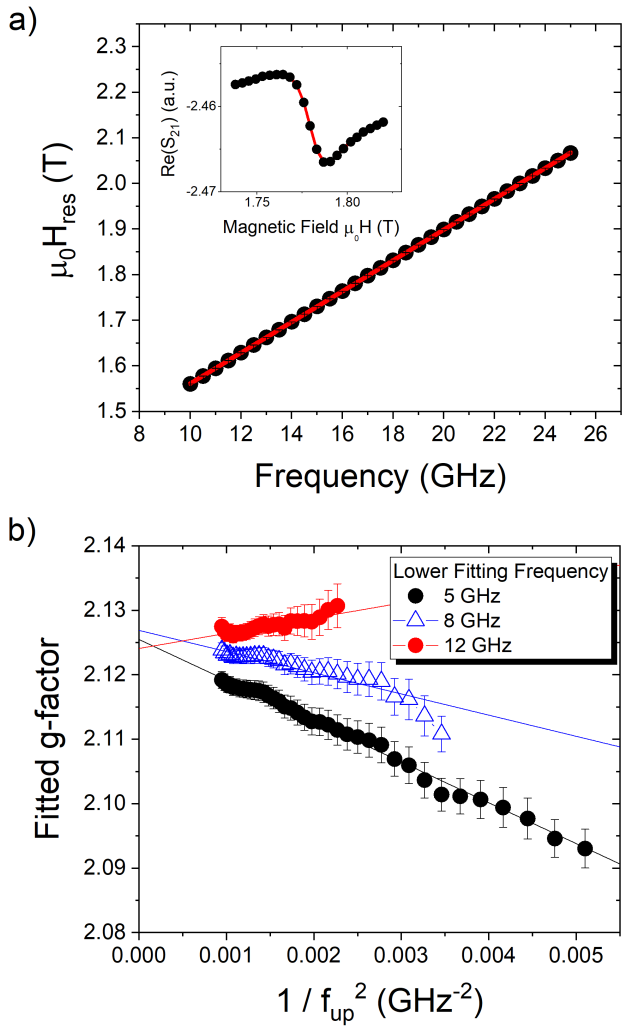

Figure S5: a) Resonance field vs. frequency for the unoxidized $Cu/Co_{90}Fe_{10}$ control sample. The red line is a fit to the data with the Kittel equation. The inset shows the real part of the S21 transmission parameter for a microwave frequency of 16.5 GHz along with a fit to the data (red line). *b) Asymptotic analysis of the g-factor for the 55s oxidized $Pt/Co_{90}Fe_{10}$ sample.*

H_k normalized to a 1 nm thickness of the ferromagnet

The anisotropy mainly originates from the two interfaces. In the same way we normalized the DMI shown in Fig. S4, we normalized H_k for the Cu/$Co_{90}Fe_{10}$ samples series to a ferromagnet with a thickness of 1 nm. The proportionality between H_k and the orbital asymmetry remains unchanged, see Fig. S6.

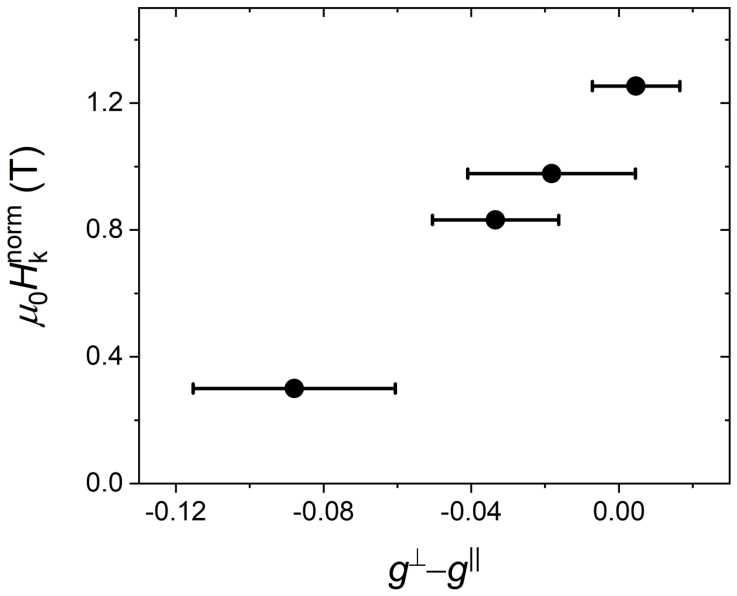

Figure S6: The normalized perpendicular anisotropy H_k^{norm} for the Cu/$Co_{90}Fe_{10}$ sample shows a linear dependence on the difference of the spectroscopic g-factor for the out-of-plane geometry and the in-plane geometry very similar to the not normalized value of H_k.

Dependence of $g^{||}$ on the oxidation

We determined $g^{||}$ for both sample series from FMR measurements. The results are shown in Fig. S7 and the error bars are significantly larger than for $g^{\perp}$.

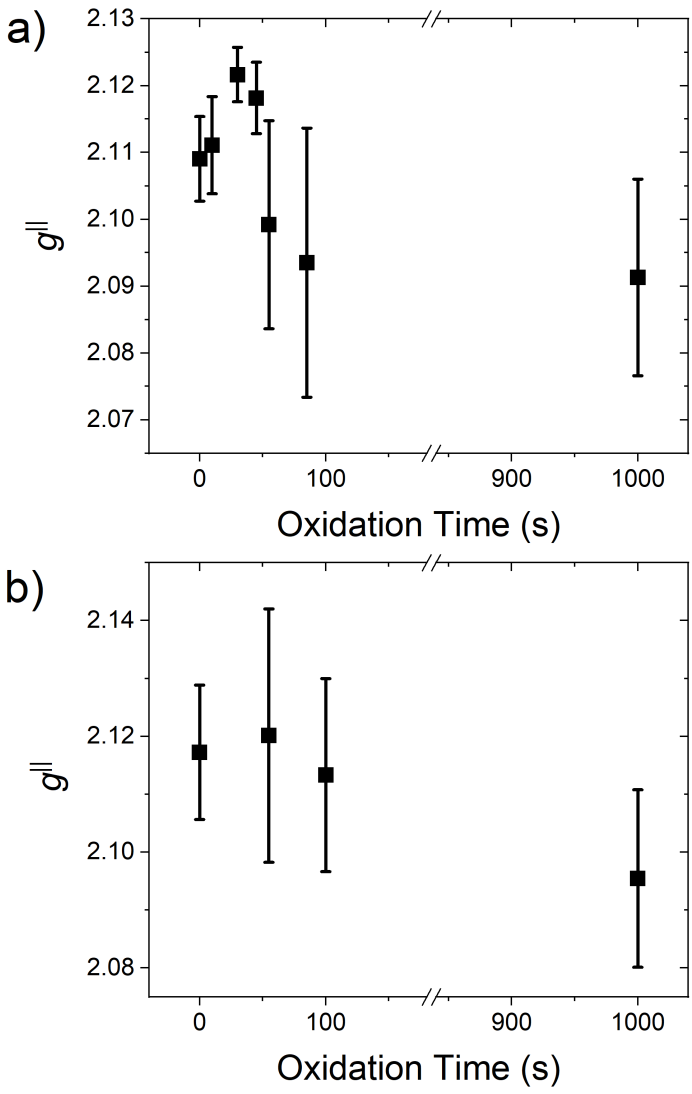

Figure S7: $g^{||}$ for a) the Pt/$Co_{90}Fe_{10}$ and b) for the Cu/$Co_{90}Fe_{10}$ sample series.